

Potential energy surfaces and properties of the Br–HBr complex

Markus Meuwly and Jeremy M. Hutson*

Department of Chemistry, University of Durham, South Road, Durham, UK DH1 3LE

Received 20th September 1999, Accepted 1st November 1999

Semiempirical potential energy surfaces for Br–HBr are constructed, based on empirical Kr–HBr, Kr–Br and Kr–Kr potentials. The electrostatic forces due to the interaction of the quadrupole of the Br atom with the multipoles of the HBr molecule are included, and make a substantial contribution to the well depths. The potentials are presented in diabatic and adiabatic representations, with and without spin–orbit coupling. When spin–orbit coupling is included, the adiabatic well depth is 342 cm^{-1} , at a linear Br–H–Br configuration. Fully coupled bound-state calculations are carried out, and the ground state is found to be bound by 269 cm^{-1} . If the complex can be observed spectroscopically, it will provide a sensitive probe of the potential energy surfaces in the entrance and exit valleys of the Br + HBr reaction. In addition, the complex is likely to be important as a product of photodissociation of HBr in HBr dimer.

I. Introduction

Molecular complexes involving open-shell constituents are attracting increasing interest, both experimental and theoretical, because their spectra can provide detailed information on potential energy surfaces in the entrance and exit valleys of chemical reactions. Species such as Cl–HCl and F–HF are particularly interesting, because they probe the potential energy surfaces for prototype hydrogen exchange reactions such as Cl + HCl and F + HF. The complexes are relatively strongly bound because a halogen atom in a $^2P_{3/2}$ state has a quadrupole moment, which can interact with the large multipole moments of the hydrogen halide molecule.

Systems such as F + HF and Cl + HCl have a long history, and have been among the important prototypes in the development of quantum-mechanical theories of reactive scattering.¹ Duggan and Grice carried out early studies of the potential energy surfaces for the abstraction^{2,3} ($H + X_2 \rightarrow HX + X$) and exchange⁴ ($X + HX \rightarrow XH + X$) reactions. The calculations were carried out as a function of the orientation of the collision partners, and used the diatomics-in-molecules (DIM) framework.^{5,6} Other approaches used for ClHCl^{7–9} include the LEPS (London–Eyring–Polanyi–Sato) and extended LEPS methods, which share several of the advantages and disadvantages of DIM. Potentials from such schemes are generally very useful in deciding whether a specific electronic state influences the energetics in the transition-state region, and in assessing reaction barriers for the different pathways. However, they usually model the long-range interactions quite poorly because they neglect the long-range electrostatic effects.

An alternative semiempirical approach, valid for X–HX complexes at long range where the HX molecule retains its identity, has been developed by Dubernet and Hutson¹⁰ and applied to Cl–HCl¹⁰ and F–HF.¹¹ This method takes the potential anisotropy from the near-isoelectronic rare gas–hydrogen halide and rare gas–halogen atom potentials, and supplements it with the correct long-range electrostatic forces involving the atomic quadrupole. The resulting surfaces have quite substantial minima, 383 and 317 cm^{-1} deep for Cl–HCl and F–HF, respectively. These minima support bound states that are attractive candidates for spectroscopy, and also have substantial effects on the reactive scattering, especially on the positions of resonances.^{12,13}

Ab initio calculations can be performed on the XHX systems, but have mostly focused on structures and energetics of the potential minima and the transition states; they have rarely mapped out substantial areas of the potential energy surfaces. This is mainly because of the very considerable computational demands such a system presents. There are three potential energy surfaces that correlate with the ground 2P state of the halogen atom, and a complete description of the dynamics requires not only the potential surfaces themselves but also the non-adiabatic and spin–orbit couplings between them. In addition, correlation effects are large, and extensive basis sets are needed to describe the relatively weak interactions in the van der Waals wells. The most complete treatment to date is a recent study of Cl–HCl by Dobbyn *et al.*,¹⁴ which includes all the major effects (but still neglects relativistic corrections).

X–HX complexes are also topical because of recent experiments by Wittig and coworkers,^{15,16} who photodissociate HX molecules in HX dimers. One of the important products is the X–HX complex, formed when an H atom is ejected from the HX dimer but the X atom does not have enough momentum to escape. In the most recent work, Liu *et al.*¹⁶ photodissociated HCl dimer by UV/IR double resonance and observed structures due to Cl–HCl in the kinetic energy of the departing H atom.

Systems other than Cl–HCl are accessible to spectroscopic experiments. Indeed, heavier HX molecules are more readily photodissociated. It thus seems worth while to construct model surfaces for the Br–HBr van der Waals complex, and this is the object of the present work.

This paper is structured as follows. In Section 2, the interaction potential is presented and the surfaces are compared to those for F–HF and Cl–HCl. In Section 3, the potential surfaces are used to calculate spectroscopically observable quantities, including the ground-state binding energy and far-infrared transition frequencies. The relevance of the results to photodissociation experiments is also considered. Finally, Section 4 summarizes our conclusions.

II. The interaction potential

The present work uses a Jacobi coordinate system, in which r is the Br–H distance, R is the distance from the HBr center of mass to the Br atom and θ is the angle between r and R ,

measured at the HBr center of mass (with $\theta = 0$ corresponding to the linear Br–H–Br geometry). Vibrations of the HBr monomer are not treated explicitly, and the potentials obtained here should be considered to be averages over the vibrational motion of HBr.

Open-shell complexes are more complicated than closed-shell complexes, because there are additional angular momenta due to the electron orbital motion and spin. As is customary for van der Waals complexes, lower-case letters are used here for quantities that refer to the monomers and upper-case letters for those that refer to the complex. The quantum numbers needed to describe complexes containing open-shell atoms have been discussed by Dubernet and Hutson.¹⁷ In particular, the total orbital and spin quantum numbers of the Br atom are denoted l and s , with resultant j_a and projection ω onto the intermolecular axis. The rotational angular momentum of the HBr monomer is denoted j , and its rotational constant is b . The total angular momentum of the complex is J and the corresponding rotational constant is B .

The interaction between an atom in a P state and a diatomic molecule can be described in terms of three diabatic or adiabatic (Born–Oppenheimer) surfaces in various ways.¹⁰ The dynamics involve all three surfaces and the couplings between them. Because of this, the Born–Oppenheimer surfaces themselves are not enough to understand the dynamics: additional information on the electronic wavefunctions is required to calculate the coupling matrix elements.

For dynamics calculations, it is generally convenient to use a diabatic rather than an adiabatic representation of the potentials. To a first approximation, the intermolecular interaction is too weak to mix in excited atomic orbitals of the halogen atom, and the atomic orbital angular momentum l is nearly conserved. In the absence of spin–orbit coupling, the three diabatic surfaces are those for interaction of HX with an X atom with its unpaired electron in a pure p_x , p_y or p_z orbital. The z axis is along the intermolecular vector R and the three atoms lie in the xz plane. An alternative way to view this is to introduce angles θ_a and ϕ_a that are conjugate to l and m_l : in a simple picture, θ_a and ϕ_a may be thought of as the angular coordinates of the unpaired electron. The resulting potential depends on the intermolecular distance R and three angles θ , θ_a and ϕ_a and thus bears similarities to a diatom–diatom interaction potential.

A. Model potential for Br–HBr

The method used here for the construction of semiempirical potential energy surfaces for X–HX systems has been described previously by Dubernet and Hutson,¹⁰ so only an outline is given here. The model is based on analogies with related systems, in this case Kr–Kr, Kr–HBr and Kr–Br, augmented with additional electrostatic terms.

For spectroscopic calculations, it is important to model the anisotropy of the potential as accurately as possible. In a system such as Br–HBr, both the atom and the molecule are anisotropic. It is convenient to expand the potential energy surface in much the same way as for a diatom–diatom system,¹⁸

$$V(R, \theta, \theta_a, \phi_a) = \sum_{\lambda_r \lambda_a \lambda_{12}} V_{\lambda_r \lambda_a \lambda_{12}}(R) \mathcal{F}_{\lambda_r \lambda_a \lambda_{12}} \quad (1)$$

The functions $\mathcal{F}_{\lambda_r \lambda_a \lambda_{12}}$ are explained in detail in ref. 10. They describe linear combinations of (space-fixed) spherical harmonics, weighted by the appropriate Clebsch–Gordan coefficients.

A first source of anisotropy involves terms similar to those that arise in Kr–HBr, which are essentially due to the shape of the HBr monomer. The Kr–HBr interaction is expanded as

$$V_{\text{Kr–HBr}}(R, \theta) = \sum_{\lambda_r} V_{\lambda_r}(R) P_{\lambda_r}(\cos \theta) \quad (2)$$

The Kr–HBr potential used in the present work is the H4 surface of Hutson.¹⁹ Since the Br atom is similar in size to the Kr atom, the Kr–HBr terms $V_{\lambda_r}(R)$ are carried over unchanged to Br–HBr. In the total potential (see below), these terms contribute anisotropic terms $V^{\lambda_r 0 \lambda_r}(R)$ to the Br–HBr potential.

A second source of anisotropy involves terms similar to those that exist for Kr–Br, and reflects the shape of the Br atom. The Kr–Br potential can be expanded

$$V_{\text{Kr–Br}}(R, \theta_a) = \sum_{\lambda_a=0,2} V_{\lambda_a}(R) P_{\lambda_a}(\cos \theta_a) \quad (3)$$

These contributions are also used unchanged in the complex and give rise to anisotropic terms $V^{0 \lambda_a \lambda_a}(R)$ with $\lambda_a = 0$ or 2. In the present work, the isotropic term $V_0(R)$ and anisotropic term $V_2(R)$ for Kr–Br were calculated by inverting the Morse–Morse switching function van der Waals (MMSV) potentials for the $X_{1/2}$, $I_{3/2}$ and $\Pi_{1/2}$ states obtained by Yourshaw *et al.*²⁰ from zero electron kinetic energy measurements (ZEKE) on KrBr[−].

In addition, electrostatic terms V_Q arise from the interaction of the atomic quadrupole on Br with the multipoles on HBr. These can be approximated as

$$V_Q(R, \theta, \theta_a, \phi_a) = \frac{5\sqrt{15}\Theta_a\mu_m\mathcal{F}_{123}}{2R^4} + \frac{5\sqrt{70}\Theta_a\Theta_m\mathcal{F}_{224}}{2R^5} \quad (4)$$

where μ_m and Θ_m are the permanent dipole and quadrupole moments of HBr and Θ_a is the quadrupole moment of the bromine atom; in the present work, the value $\Theta_a = 2.196a_0$ was taken from the results of Medved *et al.*,²¹ who carried out CASPT2 calculations including relativistic corrections.

The complete potential for Br–HBr is thus approximated by

$$V_{\text{Br–HBr}}(R, \theta, \theta_a, \phi_a) = V_{\text{Kr–HBr}}(R, \theta) + V_{\text{Kr–Br}}(R, \theta_a) - V_{\text{Kr–Kr}}(R) + V_Q(R, \theta, \theta_a, \phi_a) \quad (5)$$

Here, $V_{\text{Kr–Kr}}(R)$ is the Kr–Kr potential of Dham *et al.*²²

This semiempirical surface should eventually be superseded by high-level *ab initio* calculations. However, as indicated above, carrying out such calculations may be a difficult and laborious task.

B. Spin-free representation

The different ways to represent the potential energy surfaces for X–HX systems have been explained in detail in ref. 10. This section will therefore concentrate on a discussion of the results for Br–HBr and a comparison with the previous results on Cl–HCl¹⁰ and F–HF.¹¹

Fig. 1 shows the diabatic and adiabatic surfaces in the spin-free representation (neglecting spin–orbit coupling). The spin–orbit coupling in the Br atom is in fact so large that these surfaces are not particularly relevant for dynamical calculations. Nevertheless, they are worth considering here because the spin-free adiabatic surfaces are the ones that would result from an *ab initio* calculation excluding spin–orbit coupling. They are therefore included here for future comparisons.

The spin-free diabatic potentials are the diagonal elements of the Hamiltonian in a basis set of atomic functions quantized along the x , y and z axes. The p_x and p_y diabats are degenerate for $\theta = 0$ and 180° but diverge as the geometry departs from linear. They both have a pronounced double-minimum structure; their absolute minimum is at $\theta = 0$, with a well depth of 342 cm^{-1} . This is 25 cm^{-1} deeper than for F–HF, but 41 cm^{-1} shallower than for Cl–HCl. The double-minimum structure is less asymmetric for Br–HBr than for the lighter halogens, mainly because HBr has a larger quadrupole and smaller dipole than HCl and HF. For Br–HBr, the secondary minimum in the p_x and p_y diabats is only 35 cm^{-1} shallower than the primary minimum.

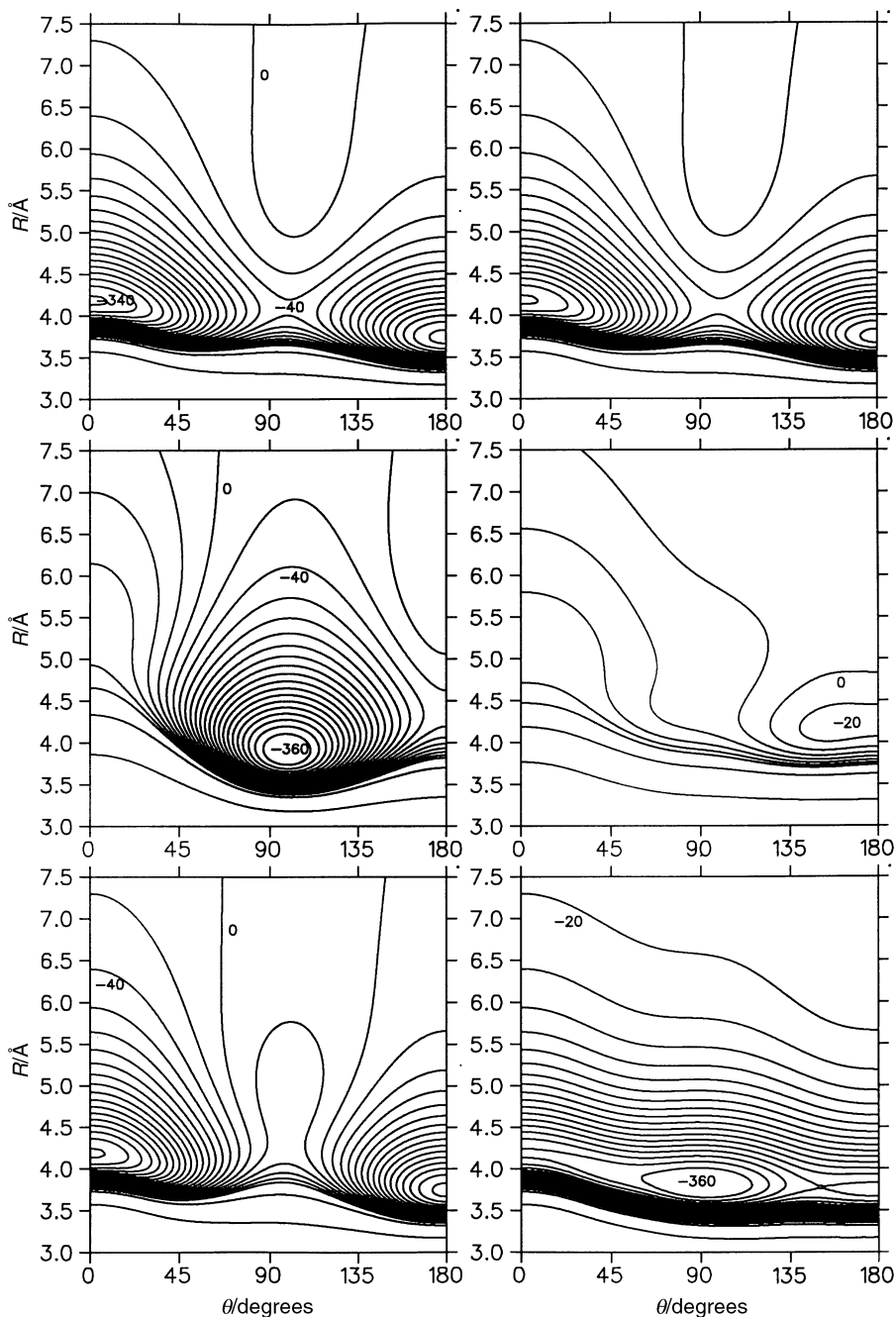


Fig. 1 Contour plot of the interaction potential excluding spin. Diabatic potentials (p_y , p_z , p_x from top to bottom) are shown on the left, adiabatic ones ($1A'$, $2A'$, $1A'$ from top to bottom) on the right-hand side. Contours are drawn every 20 cm^{-1} up to $+100 \text{ cm}^{-1}$ and at 200 and 1000 cm^{-1} .

The minimum energy structure on the p_z diabat is close to $\theta = 90^\circ$. Again, the surface is more nearly symmetric around $\theta = 90^\circ$ than for F–HF and Cl–HCl, for the same reason. The T-shaped minimum can be explained by purely electrostatic considerations: the partially filled p_z orbital produces a quadrupole on the Br atom which interacts favourably with the substantial quadrupole of HBr.

The potential energy surfaces can be expressed in an adiabatic form by diagonalizing the matrix representation of the potential in the basis set of atomic functions. The transformation leaves the p_y surface unchanged but mixes the p_x and p_z potentials through the off-diagonal elements described in ref. 10. The diagonalization produces two surfaces of A' symmetry and one of A'' symmetry. The minimum of the lowest adiabat ($1A'$) is in a T-shaped configuration with a well depth of 387 cm^{-1} . This is qualitatively different from Cl–HCl and F–HF, where there were both linear and T-shaped minima but the

linear minimum was slightly deeper. The upper A' diabat ($2A'$) has only a very shallow minimum (98 cm^{-1} deep) at the Br–Br–H geometry, and is repulsive over most of the angular range.

C. Representation including spin

Either the spin–orbit coupling in the Br atom can be regarded as coupling the spin-free states, or it can be included in the description of the potential surfaces. In Br–HBr, the spin–orbit coupling is so large that the latter is physically more sensible. To do this, we assume that the spin–orbit coupling in the complex is the same as in the isolated Br atom, and is of the form $\xi \hat{J} \cdot \hat{s}$, where $\xi = -2457 \text{ cm}^{-1}$. The matrix representation is constructed in a basis set of atomic orbital functions for $l = 1$ and spin functions for $s = 1/2$, with resultant $j_a = 1/2$ or $3/2$ and projection ω onto the intermolecular axis. The

resulting 6×6 matrix has three pairs of equal diagonal elements and three doubly degenerate pairs of eigenvalues; either the diagonal elements (diabats) or the eigenvalues (adiabats) can be plotted. Contour plots of the resulting surfaces are shown in Fig. 2.

Two diabatic surfaces correspond to $j_a = 3/2$ with $|\omega| = 3/2$ and $1/2$ and one to $j_a = 1/2$, $|\omega| = 1/2$. The last is shifted upwards at long range by the atomic spin-orbit splitting, $3/2|\xi|$. The two $j_a = 3/2$ diabats are qualitatively (but not quantitatively) similar to the p_x and p_z diabats. As for F-HF and Cl-HCl, however, the $j_a = 1/2$, $|\omega| = 1/2$ diabats is quite different from any of the spin-free diabats. This is because an atomic state with $j_a \leq 1$ cannot have an overall quadrupole moment. The attractive electrostatic components thus make no contribution to the $j_a = 1/2$ diabats, and its anisotropy stems solely from that of the Kr-HBr potential.

The right-hand side of Fig. 2 shows the adiabatic surfaces obtained when spin-orbit coupling is included. There are

again two surfaces that correlate at long range with Br ($^2P_{3/2}$) and one that correlates with Br ($^2P_{1/2}$). On the lowest adiabat, Br-HBr has minima in both linear configurations. The wells are 342 cm^{-1} deep for Br-HBr and 307 cm^{-1} deep for Br-BrH. By contrast, F-HF shows minima in the linear and a near-T-shaped conformation, and for Cl-HCl the secondary minimum is almost washed out. The different behaviour for Br-HBr occurs partly because of the larger quadrupole moment of HBr and partly because of the deeper secondary minimum in Kr-HBr (which itself arises because the Br atom in HBr has a strongly anisotropic repulsion, with a "dent" in the electron density at the point furthest from the H atom).

The second adiabat for Br-HBr also has a double-minimum structure, with its absolute minimum (98 cm^{-1}) at the Br-BrH structure. The highest-lying adiabat, which correlates with Br ($^2P_{1/2}$), is quite similar to its diabatic $j_a = 1/2$, $|\omega| = 1/2$ counterpart, because the large spin-orbit splitting in Br prevents efficient mixing.

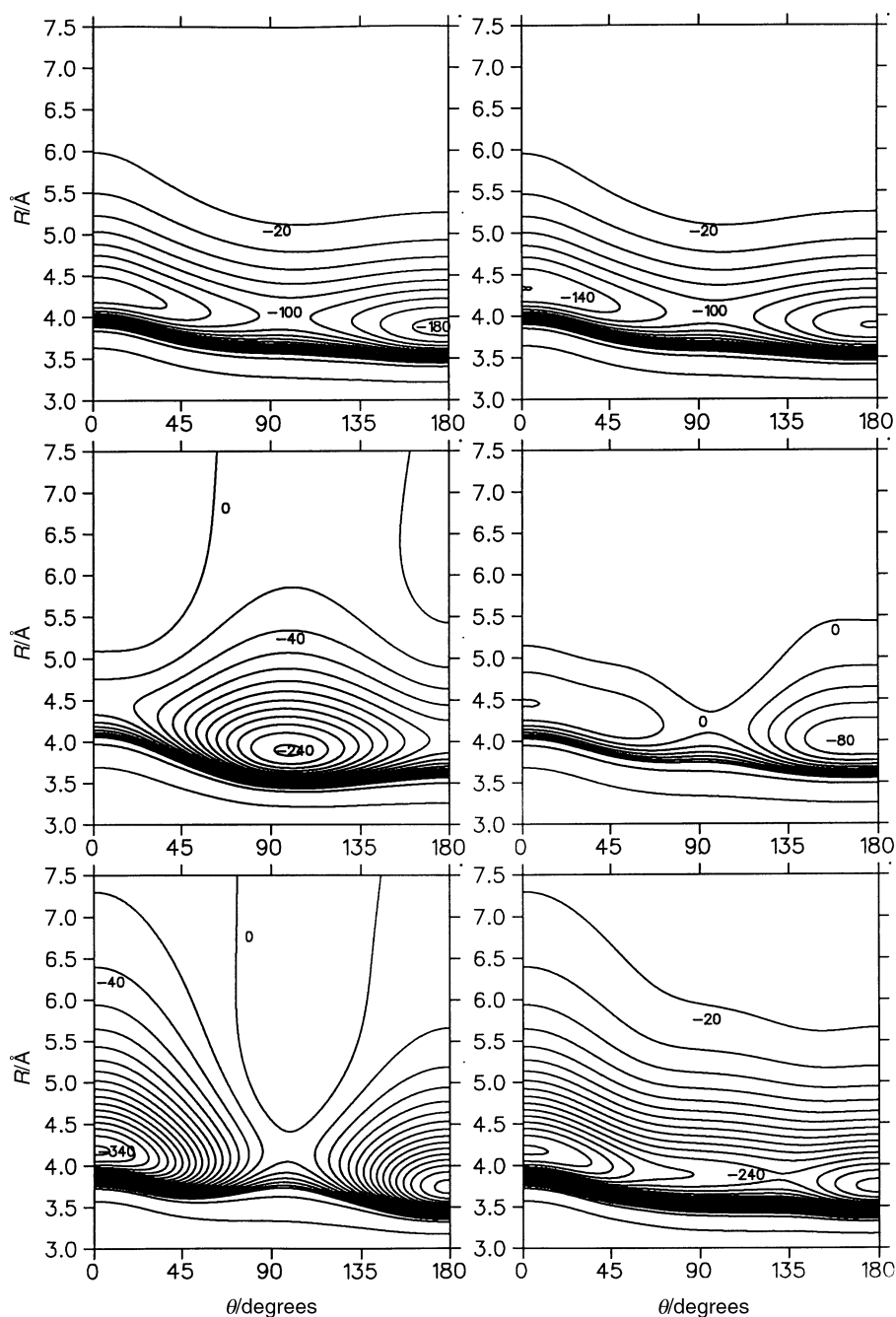


Fig. 2 Contour plot of the interaction potential including spin. Diabatic surfaces $[(j_a, \omega) = (1/2, 1/2), (3/2, 1/2), (3/2, 3/2)]$ from top to bottom are shown on the left, adiabatic ones on the right-hand side. Contours are drawn every 20 cm^{-1} up to $+100 \text{ cm}^{-1}$ and at 200 and 1000 cm^{-1} .

III. Spectroscopy and dynamics

The present interaction potentials make it possible to calculate several properties of experimental interest. We begin with the bound states. We have performed close-coupling calculations to locate the lowest few states of Br–HBr, using the BOUND package.^{23,24} The methods used are the same as in ref. 10. All three surfaces and all the couplings between them are included. The HBr molecule in the complex is treated as a rigid rotor with a rotational constant $b = 8.35106 \text{ cm}^{-1}$. All monomer rotational functions up to $j = 15$ are included. The reduced mass of the Br–HBr complex is taken to be $39.709508 m_u$ [where $m_u = m_a(^{12}\text{C})/12$]. The coupled equations are propagated from $R_{\min} = 2 \text{ \AA}$ to $R_{\max} = 8 \text{ \AA}$ and the results are extrapolated to zero step size using Richardson h^4 extrapolation.

The ground state can be regarded as a bending state of a linear molecule with bending quantum number $v_b = 0$, vibrational angular momentum $k = 0$ and $|\omega| = 3/2$. As for Cl–HCl and F–HF, it has total angular momentum $J = 3/2$, with projection $|P| = 3/2$ onto the intermolecular axis. For Br–HBr, the ground state lies 268.78 cm^{-1} below dissociation to $\text{Br}(^2\text{P}_{3/2}) + \text{HBr}$. This binding energy is about 5 cm^{-1} less than for Cl–HCl and 95 cm^{-1} more than for F–HF. Excitation of the bending vibration $v_b = 1$ leads to two states with $|P| = 1/2$ and $5/2$ (corresponding to vibrational angular momentum $k = \pm 1$). They are found 34 cm^{-1} and 56 cm^{-1} , respectively, above the ground state and transitions to them may be detectable in the far-infrared.

A further quantity of interest is the lifetime of the quasi-bound states correlating with $\text{Br}(^2\text{P}_{1/2})$. Such lifetimes have been calculated for the lowest $j_a = 1/2$ states of F–HF (583 ps) and Cl–HCl (277 ns),¹¹ using the MOLSCAT program.²⁵ The difference arises because the larger spin–orbit splitting in Cl–HCl results in a much larger energy release, which requires more HX rotation in the products to accommodate it; the HF product from F–HF is generated mostly in $j = 3$, whereas the HCl product from Cl–HCl is generated mostly in $j = 8$. However, Br–HBr is more complicated. If the calculations are performed using rigid-rotor HBr, the predissociating state is found at an energy 3560.76 cm^{-1} above the $\text{Br}(^2\text{P}_{3/2}) + \text{HBr}$ dissociation limit, with a width of $3.6 \times 10^{-8} \text{ cm}^{-1}$, corresponding to a lifetime of 15 ms. This is indeed orders of magnitude longer than for F–HF or Cl–HCl. However, this state lies above the threshold for production of vibrationally excited HBr, and predissociation to form this is likely to be the dominant process. Unfortunately, calculating the rate of this process would require a more sophisticated (r -dependent) potential than we have at present. Nevertheless, we can make an estimate. The highest energetically accessible ro-vibrational channel of HBr is $v = 1, j = 12$. Predissociation of $\text{Br}(^2\text{P}_{1/2})\text{--HBr}$ to form such products still involves more rotational excitation than is necessary in Cl–HCl, so it is likely that the state for Br–HBr will have a lifetime longer than for Cl–HCl.

The present potentials are also relevant to the photodissociation experiments of Wittig and coworkers,^{15,16} who photodissociate HX molecules in HX dimers with ultraviolet light and monitor the kinetic energy of the H atoms ejected. They have so far carried out experiments on HI dimer¹⁵ and HCl dimer.¹⁶ For HCl dimer, they identified peaks in the kinetic energy distribution corresponding to production of Cl–HCl on each of the three adiabatic surfaces (including spin). Because of the mass ratios, only a very small fraction (about 1 part in 70) of the excess energy is deposited in the internal motions of the Cl–HCl complex. For HBr dimer, this fraction will be even smaller (about 1 part in 160). There is thus a very good chance that Br–HBr complexes will be formed in bound states. The present surfaces will be valuable in interpreting such experiments.

IV. Conclusions

We have presented model potential energy surfaces for the Br–HBr complex, valid at van der Waals distances where the HBr molecule retains its identity in the complex. There are three potential energy surfaces that correlate with $\text{Br}(^2\text{P})$, which can be described in either diabatic or adiabatic and either spin-free or spin-containing representations. All three surfaces, and the couplings between them, are needed for an adequate treatment of the spectroscopy and dynamics.

The Br–HBr complex is much more strongly bound than the near-isoelectronic Kr–HBr, because the Br atom possesses a quadrupole moment that interacts electrostatically with the permanent multipole moments of the HBr molecule.

The most physically realistic representation is the spin-containing adiabatic one. For this, our lowest surface has a linear equilibrium geometry, Br–H–Br, with a well depth of 342 cm^{-1} . The lowest bound state has a binding energy of 269 cm^{-1} , and far-infrared transitions originating in it are predicted near 34 and 56 cm^{-1} .

The surfaces developed here are valid at long range, but do not extend correctly to the transition-state region. The development of global potential energy surfaces would require either extensive *ab initio* calculations or combining the present surfaces with reactive surfaces in the same spirit as the work of Maierle *et al.*¹² for Cl–HCl. The present surfaces neglect any chemical bonding effects; there is some evidence that such effects are significant around $\theta = 90^\circ$ for F–HF,²⁶ and the same may be true for Br–HBr. If so, the well depth of the lowest spin-free adiabat may be somewhat deeper than the present work suggests.

The potential energy surfaces developed here should also assist in understanding the results of photodissociation experiments such as those of Wittig and coworkers, in which an HBr molecule is photodissociated in HBr dimer to form products that include Br–HBr.

Acknowledgements

M.M. acknowledges financial support from the Schweizerischer Nationalfonds zur Förderung der wissenschaftlichen Forschung. The calculations were carried out on a Silicon Graphics Origin 2000 computer system, which was purchased with funding from the Engineering and Physical Sciences Research Council. We are grateful to Dr. Lydia Heck for computational assistance.

References

- 1 G. C. Schatz, D. Sokolovski and J. N. L. Connor, *Adv. Mol. Vibrat. Collision Dynam.*, 1994, **2B**, 1.
- 2 J. J. Duggan and R. Grice, *J. Chem. Phys.*, 1983, **78**, 3842.
- 3 J. J. Duggan and R. Grice, *J. Chem. Soc., Faraday Trans.*, 1984, **80**, 729.
- 4 J. J. Duggan and R. Grice, *J. Chem. Soc., Faraday Trans.*, 1983, **80**, 739.
- 5 F. O. Ellison, *J. Am. Chem. Soc.*, 1963, **85**, 3540.
- 6 J. C. Tully, *Adv. Chem. Phys.*, 1980, **42**, 63.
- 7 D. K. Bondi, J. N. L. Connor, J. Manz and J. Römel, *Mol. Phys.*, 1983, **50**, 467.
- 8 A. Persky and H. Kornweitz, *J. Phys. Chem.*, 1987, **91**, 5496.
- 9 H. Kornweitz, M. Broida and A. Persky, *J. Phys. Chem.*, 1989, **93**, 251.
- 10 M.-L. Dubernet and J. M. Hutson, *J. Phys. Chem.*, 1994, **98**, 5844.
- 11 M. Meuwly and J. M. Hutson, *J. Chem. Phys.*, 2000, **112**, in press.
- 12 C. S. Maierle, G. C. Schatz, M. S. Gordon, P. McCabe and J. N. L. Connor, *J. Chem. Soc., Faraday Trans.*, 1997, **93**, 709.
- 13 G. C. Schatz, P. McCabe and J. N. L. Connor, *Faraday Discuss. Chem. Soc.*, 1998, **110**, 139.
- 14 A. J. Dobbyn, J. N. L. Connor, N. A. Besley, P. J. Knowles and G. C. Schatz, *Phys. Chem. Chem. Phys.*, 1999, **1**, 957.
- 15 J. Zhang, M. Dulligan, J. Segall, Y. Wen and C. Wittig, *J. Phys. Chem.*, 1995, **99**, 13680.

- 16 K. Liu, A. Kolessov, J. W. Partin, I. Bezel and C. Wittig, *Chem. Phys. Lett.*, 1999, **299**, 374.
- 17 M.-L. Dubernet and J. M. Hutson, *J. Chem. Phys.*, 1994, **101**, 1939.
- 18 C. G. Gray, *Can. J. Phys.*, 1968, **46**, 135.
- 19 J. M. Hutson, *J. Chem. Phys.*, 1989, **91**, 4455.
- 20 I. Yourshaw, T. Lenzer, G. Reiser and D. M. Neumark, *J. Chem. Phys.*, 1998, **109**, 5247.
- 21 M. Medved, P. W. Fowler and J. M. Hutson, *Mol. Phys.*, 2000, in press.
- 22 A. K. Dham, A. R. Allnatt, W. J. Meath and R. A. Aziz, *Mol. Phys.*, 1989, **67**, 1291.
- 23 J. M. Hutson, BOUND computer program, version 5, distributed by Collaborative Computational Project No. 6 of the UK Engineering and Physical Sciences Research Council, 1993.
- 24 J. M. Hutson, *Comput. Phys. Commun.*, 1994, **84**, 1.
- 25 J. M. Hutson and S. Green, MOLSCAT computer program, version 14, distributed by Collaborative Computational Project No. 6 of the UK Engineering and Physical Sciences Research Council, 1994.
- 26 M. Bittererová and S. Biscupič, *Chem. Phys. Lett.*, 1999, **299**, 145. Note that in Table 5 the second column should be headed R_{HF^+} , and that all the energies should be negative.

Paper a907611e